

# Non-Gaussianity of the Cosmic Baryon Fluid: Log-Poisson Hierarchy Model

Ji-Ren Liu and Li-Zhi Fang

*Department of Physics, University of Arizona, Tucson, AZ 85721*

## ABSTRACT

In the nonlinear regime of cosmic clustering, the mass density field of the cosmic baryon fluid is highly non-Gaussian. It shows different dynamical behavior from collisionless dark matter. Nevertheless, the evolved field of baryon fluid is scale-covariant in the range from the Jeans length to a few ten  $h^{-1}$  Mpc, in which the dynamical equations and initial perturbations are scale free. We show that in the scale-free range, the non-Gaussian features of the cosmic baryon fluid, governed by the Navier-Stokes equation in an expanding universe, can be well described by a log-Poisson hierarchical cascade. The log-Poisson scheme is a random multiplicative process (RMP), which causes non-Gaussianity and intermittency even when the original field is Gaussian. The log-Poisson RMP contains two dimensionless parameters:  $\beta$  for the intermittency and  $\gamma$  for the most singular structure. All the predictions given by the log-Poisson RMP model, including the hierarchical relation, the order dependence of the intermittent exponent, the moments, and the scale-scale correlation, are in good agreement with the results given by hydrodynamic simulations of the standard cold dark matter model. The intermittent parameter  $\beta$  decreases slightly at low redshift and indicates that the density field of baryon fluid contains more singular structures at lower redshifts. The applicability of the model is addressed.

*Subject headings:* cosmology: theory - large-scale structure of universe

## 1. Introduction.

In the universe, about 72% of the energy density is in the form of dark energy, 24% cold dark matter, and a small fraction, 4% baryon matter. Since the dark energy is assumed to be spatially uniform, the dynamics of the clustering of cosmic baryon fluid should be dominated by the underlying gravitational potential of dark matter. However, it has already been recognized in the early study of cosmic structure formation that in the nonlinear regime the

dynamical behavior of the cosmic baryon fluid, or of the intergalactic medium (IGM), doesn't always follow the collisionless dark matter. Although the cosmic baryon fluid is passive substance in comparing with dark matter, it statistically decouples from the underlying dark matter field in the non-linear evolutionary stage. In the scale free range, the cosmic baryon fluid, as a Navier-Stokes fluid in the expanding universe, is similar to the fluid being moved by inertia, and should show some features as the turbulence in inertial range (Shandarin and Zeldovich 1989).

Later, it was found that the dynamical equations of the velocity fields of cosmic matter essentially are a variant of the random-force-driven Burgers' equation (Gurbatov et al. 1989; Berera & Fang 1994). For baryon fluid, it is a Burgers' equation driven by the random force of the gravity of dark matter (Jones 1999; Matarrese & Mohayaee 2002). Burgers' fluid will show highly non-Gaussian features due to the development of Burgers' turbulence when the Reynolds number is large enough (Polyakov 1995; Lässig 2000; Bec & Frisch 2000; Davoudi et al. 2001). In this state, the Burgers' fluid consists of shock waves in low as well as in high density regions, and therefore, non-Gaussianity can be seen in low as well as in high density regions.

This property has received supports from the absorption spectra of QSOs, which is caused by the IGM with moderate mass density. For example, the Ly $\alpha$  transmitted flux in the absorption spectra of QSOs is found to be significantly intermittent and its probability distribution functions (PDF) are remarkably long tailed (Jamkhedkar et al. 2000; Pando et al. 2002; Feng et al. 2003). The H I and He II Ly $\alpha$  absorption lines of QSO HE2347 can not be explained by thermal broadening, but consistent with turbulence broadening (Zheng et al. 2004; Liu et al. 2006). Moreover, samples produced by cosmological hydrodynamic simulations also reveal the statistical decoupling of baryon matter from dark matter and the non-Gaussian features of Burgers' turbulence (He et al. 2004, 2005; Kim et al. 2005).

One of the latest developments in this direction is that the random velocity fields of the cosmic baryon fluid are found to be extremely well described by She-Leveque's (SL) scaling formula (She & Leveque 1994) in the scale range from the Jeans length to larger than  $10 h^{-1}$  Mpc (He et al. 2006). The SL scaling formula is believed to characterize the scaling hierarchy of the non-linear evolution of Navier-Stokes fluid, like fully developed turbulence (e.g., Frish 1995). Therefore, the dynamical features of the cosmic baryon fluid in the nonlinear regime are similar to the fully developed turbulence: it is of scaling hierarchy. It is interesting to note that the SL formula has also been successfully applied to describe the mass fields of gas on interstellar scales (Boldyrev et al. 2002; Padoan et al. 2003).

The SL formula actually is originated from a cascade of log-Poisson random multiplicative process (RMP), which is related to the hidden symmetry of the Navier-Stokes equations

(Dubrulle 1994; She & Waymire 1995; Benzi et al. 1996). This motivate us to investigate whether the clustering behavior of the mass density field of the cosmic baryon fluid can be described by the log-Poisson RMP. Theoretically, this is not trivial, because the cosmic baryon fluid is compressible and dominated by the gravitational field of dark matter, while the SL scaling formula originally was proposed to describe the velocity field of incompressible fluid.

The paper is organized as follows. §2 describes the model of the log-Poisson RMP for the nonlinear evolution of the cosmic baryon fluid. The predictions and its tests of the log-Poisson RMP model are presented in §3. §4 presents briefly the redshift-evolution of the coefficients of the log-Poisson model. Discussion and conclusion are given in §5.

## 2. Log-Poisson RMP model

### 2.1. The log-Poisson hierarchy

The clustering and non-Gaussianity of the cosmic mass density and velocity fields are usually measured by two and multiple point correlation functions. To reveal the features of the scaling hierarchy of the mass density field, however, it is more effective to use the structure function defined by

$$S_p(r) \equiv \langle |\delta\rho_r|^p \rangle, \quad (1)$$

where  $\delta\rho_r = \rho(\mathbf{x} + \mathbf{r}) - \rho(\mathbf{x})$ ,  $r = |\mathbf{r}|$ ,  $p$  is the order of statistics, and the average  $\langle \dots \rangle$  is taken over the ensemble of density field. For statistically isotropic and homogenous random field  $\rho(\mathbf{x})$ ,  $S_p(r)$  depends only on  $r$ .

The difference between the correlation function and structure function has been analyzed in detail by Monin & Yaglom (1975). The variable  $\delta\rho_r = \rho(\mathbf{x} + \mathbf{r}) - \rho(\mathbf{x})$  is not  $\delta\rho(\mathbf{x}) = \rho(\mathbf{x}) - \bar{\rho}$ ,  $\bar{\rho}$  being the mean of density; the variable  $\delta\rho(\mathbf{x})$  can be larger than  $\bar{\rho}$ , but cannot be less than  $-\bar{\rho}$ , and therefore, for a nonlinear field, the distribution of  $\delta\rho(\mathbf{x})$  generally is skew; however, the distribution of  $\delta\rho_r$  is symmetric with respect to positive and negative  $\delta\rho_r$  if the field is statistically uniform.

In the scale-free range of the fluid, the structure function as a function of  $r$  can be expressed as a power law

$$S_p(r) \propto r^{\xi(p)}. \quad (2)$$

For fully developed turbulence of Navier-Stokes fluid,  $\xi(p)$  is a nonlinear function of  $p$ , i.e. the mass field is intermittent, and  $\xi(p)$  is called intermittent exponent (Frisch 1995). Since the pioneer work of Kolmogorov (1941), it is believed that the relation of  $\xi(p)$  vs.  $p$  is

related to the scale-covariance of the dynamical equations and initial conditions. Since then many hierarchy models for interpreting  $\xi(p)$  have been proposed. Finally the best model is given by the SL scaling formula (She & Leveque 1994). It has been shown that the SL formula is yielded from the Log-Poisson hierarchy process, which is related to the so-called generalized scale covariance of the Navier-Stokes equations (Dubrulle 1994). Therefore, one may expect that the statistical behavior of the mass field of cosmic baryon matter would also be interpreted by the log-Poisson random multiplicative processes (RMP).

The log-Poisson RMP assumes that, in the scale-free range, the variables  $|\delta\rho_r|$  on different scales  $r$  are related from each other by a statistically hierarchy relation given by

$$|\delta\rho_{r_2}| = W_{r_1 r_2} |\delta\rho_{r_1}|, \quad (3)$$

where

$$W_{r_1 r_2} = \beta^m (r_1/r_2)^\gamma, \quad (4)$$

which describes how the fluctuation  $|\delta\rho_{r_1}|$  on the larger scale  $r_1$  related to fluctuations  $|\delta\rho_{r_2}|$  on the smaller scale  $r_2$ . In eq.(4),  $m$  is a Poisson random variable with the PDF

$$P(m) = \exp(-\lambda_{r_1 r_2}) \lambda_{r_1 r_2}^m / m!. \quad (5)$$

To insure the normalization  $\langle W_{r_1 r_2} \rangle = 1$ , where  $\langle \dots \rangle$  is over  $m$ , the mean  $\lambda_{r_1 r_2}$  of the Poisson distribution should be

$$\lambda_{r_1 r_2} = \gamma [\ln(r_1/r_2)] / (1 - \beta). \quad (6)$$

It is enough to consider only  $|\delta\rho_r|$ , as the distribution of positive and negative  $\delta\rho_r$  is symmetric.

The log-Poisson model of equation (3) depends only on the ratio  $r_1/r_2$ , thus, it is scale invariant. The model is determined by two dimensionless positive parameters:  $\beta$  and  $\gamma$ , of which the physical meaning will be given below. Equation (3) relates  $\delta\rho_r$  on different scales by multiplying a random factor  $W$ , and therefore, it is a random multiplicative process (RMP), which generally yields a non-Gaussian field even when the field originally to be Gaussian (Pando et al. 1998). For a Gaussian field, variables  $\delta\rho_{r_1}$  and  $\delta\rho_{r_2}$  are statistically independent and it requires  $\beta \rightarrow 1$  in equation (4).

## 2.2. Parameter $\gamma$ and singular structures

With the log-Poisson model, the intermittent exponent  $\xi(p)$  is given by (see Appendix)

$$\xi(p) = -\gamma [p - (1 - \beta^p) / (1 - \beta)]. \quad (7)$$

For a Gaussian field with scale-free power spectrum, we have  $\xi(p) \propto p$ . This indicates again that a Gaussian field requires  $\beta \rightarrow 1$ .

Considering a density field containing singular structures at positions  $\mathbf{x}_i$ , we have  $\rho(\mathbf{x}) \propto |\mathbf{x} - \mathbf{x}_i|^{-\alpha}$  near  $\mathbf{x}_i$  with  $\alpha > 0$ . The variables  $|\delta\rho_r|^p$  near  $\mathbf{x}_i$  should be  $\simeq |r|^{-\alpha p}$ , and therefore  $|\delta\rho_r|^{p+1}/|\delta\rho_r|^p \simeq |r|^{-\alpha}$ . Thus, to pick up the singular structures, we define a statistical tool as

$$F_p(r) \equiv S_{p+1}(r)/S_p(r). \quad (8)$$

For higher  $p$ , singular structures have larger contributions to  $S_p(r)$ , while for lower  $p$ , weak-clustering structures have larger contributions to  $S_p(r)$ . Therefore  $F_p(r)$  measures clustering structures, which are dominant for the  $p$ -order statistics. Obviously, when  $p \rightarrow \infty$ ,  $F_p(r)$  should be dominated by the singular structures, i.e.,  $F_\infty \propto r^{-\alpha}$ .

On the other hand, from equations (2), (7), and (8), one finds

$$F_p(r) \propto r^{-\gamma(1-\beta^p)}. \quad (9)$$

Since  $\beta < 1$ , we have

$$F_\infty = \lim_{p \rightarrow \infty} \frac{\langle |\delta\rho_r|^{p+1} \rangle}{\langle |\delta\rho_r|^p \rangle} \propto r^{-\gamma}. \quad (10)$$

Therefore, the parameter  $\gamma$  of the log-Poisson RMP is actually the power-law index of the mass profile of the most singular structures. It should be pointed out that the word ‘‘singular’’ is applicable only asymptotically, because we cannot let  $r \rightarrow 0$  to pick up the singular structure, as  $r$  should be in the scale-free range.

### 2.3. Parameter $\beta$ and intermittency

As mentioned in last subsection, when  $\beta \rightarrow 1$ , the field would be Gaussian, and therefore, equation (9) implies that for a Gaussian field,  $F_p(r)$  would be  $r$ -independent. On the other hand, for a utmost intermittent field, which consists only the most singular structures, and the fluctuations between the singular structures are zero,  $F_p(r)$  should be equal to  $r^{-\gamma}$  regardless of  $p$ . From equation (9), the utmost intermittent field should have  $\beta = 0$ . Thus, the parameter  $\beta$  is to measure the level of intermittency: non-intermittency corresponds to  $\beta = 1$ , and the strongest intermittency corresponds to  $\beta = 0$ .

The meaning of  $\beta$  can also be seen with the following hierarchical relation of  $F_p(r)$

$$\frac{F_p(r)}{F_\infty(r)} = \left[ \frac{F_{p+1}(r)}{F_\infty(r)} \right]^{1/\beta}, \quad (11)$$

which can be derived from equations (9) and (10). Equation (11) is invariant with respect to a translation in  $p$ . In deriving eq.(11), we assume that the proportional coefficient of equation (9) is  $p$ -independent. We will show that this assumption is correct.

As mentioned in §2.2, the  $F_p(r)$  measures the clustered structures dominating the  $p$  order statistics. The smaller the  $p$ , the larger the contribution of weak-clustering structures to  $F_p(r)$ . Therefore, equation (10) describes the hierarchical relation between the stronger (or high  $p$ ) and weaker (or low  $p$ ) clustering. In the scale-free range where  $F_{p+1}(r)/F_\infty(r) < 1$ , we have  $F_p(r)/F_\infty(r) < F_{p+1}(r)/F_\infty(r)$  if  $\beta < 1$ . That is, for an intermittent field, weak clustering structures are strongly suppressed with respect to the most singular structures; the smaller the  $\beta$ , the stronger the suppression of weak clustering structures.

### 3. Non-Gaussianity of the cosmic baryon fluid

The samples for testing the model of §2 are similar to that used in He et al. (2006), which are given by a hybrid hydrodynamic/ $N$ -body simulation, consisting of the WENO algorithm for baryon fluid and  $N$ -body simulation for particles of dark matter (Feng et al. 2004). We now produce samples of 50  $h^{-1}$  Mpc box,  $768^3$  grid, and the cosmological parameters are taken from the results of WMAP (Spergel et al. 2006). The samples output at redshifts 0, 1, 2, 3, and 4. We randomly sample 10,000 one-dimensional sub-samples at each redshift.

In order to have a complete description of the density field and avoid false statistical correlation, the variable  $\delta\rho_r$  should be given by a proper decomposition of the field  $\rho_{\mathbf{x}}$ . We will use the decomposition of discrete wavelet transform (DWT), which is found to be effective to describe turbulence (e.g., Farge 1992). With the DWT, the variables of mass density field is given by

$$\delta\rho_r = \int \rho(\mathbf{x})\psi_{j,l}(\mathbf{x})d\mathbf{x}, \quad (12)$$

where  $\psi_{j,l}(\mathbf{x})$  is the base of discrete wavelet transform (e.g., Fang & Thews 1998). For a one-dimensional sample of length  $L$ , the scale index  $j$  is related to the scale  $r$  by  $r = L/2^j$  and the position index  $l$  is for the cell at  $\mathbf{x} = lL/2^j$  to  $(l+1)L/2^j$ . We will use the Harr wavelet to do the calculation below. We also repeat the calculations with wavelet Daubechies 4. The non-Gaussian statistical features given by Daubechies 4 are the same as that of Haar wavelet.

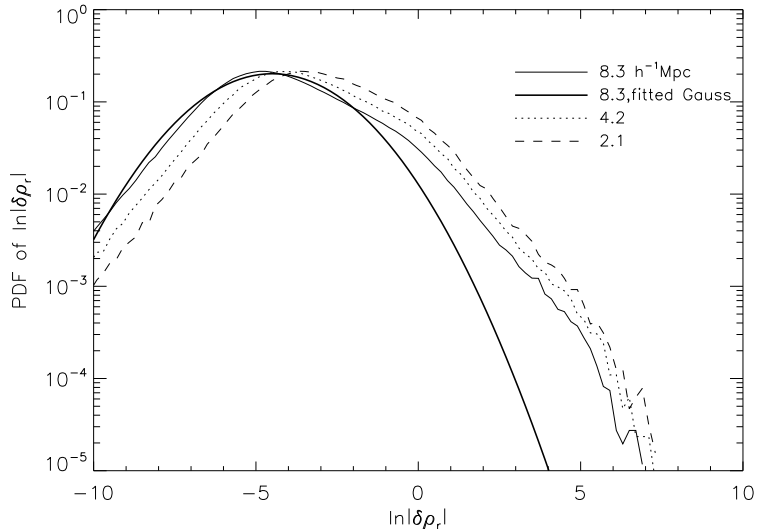


Fig. 1.— PDFs of the density difference  $\ln|\delta\rho_r|$  with  $r = 2.1, 4.2$  and  $8.3 \text{ h}^{-1} \text{ Mpc}$  for samples at  $z = 0$ . A fitted Gaussian PDF of  $\ln|\delta\rho_r|$  is also shown.

### 3.1. PDF and structure function

We first show the basic statistical deviation of the baryon mass density field from a Gaussian field. Figure 1 gives the PDF of the density difference variables,  $p(\ln|\delta\rho_r|)d\ln|\delta\rho_r|$ , for the cosmic baryon fluid sample at  $z = 0$  on scales  $r = 2.1, 4.3, 8.3 \text{ h}^{-1} \text{ Mpc}$ . A fitted Gaussian to the PDF on scale  $8.3 \text{ h}^{-1} \text{ Mpc}$  is also shown as the thick solid line in Figure 1. Since the Gaussian fitting is for  $\ln|\delta\rho_r|$ , the fitted curve actually is a lognormal distribution for  $|\delta\rho_r|$ . It shows clearly that on all the scales, the PDFs of  $|\delta\rho_r|$  are non-Gaussian and have a longer tail than the lognormal distribution.

The long tailed events can be effectively described by the  $p$ -dependence of the structure function  $S_p(r)$ . Figure 2 shows  $S_p(r)$  as a function of  $r$  for  $p = 0.5$  to  $4$  for the cosmic baryon fluid sample at  $z = 0$ . For all  $p$  the structure function  $\ln S_p(r)$  of fig. 2 can be well fitted by a straight line in the scale range of  $2 \leq r \leq 16 \text{ h}^{-1} \text{ Mpc}$ . The data points at  $1 \text{ h}^{-1} \text{ Mpc}$  are slightly deviating from the straight line given by the fitting over  $2 \leq r \leq 16 \text{ h}^{-1} \text{ Mpc}$ , because  $1 \text{ h}^{-1} \text{ Mpc}$  is already close to the Jeans length. We only focus on the range of  $2 \leq r \leq 16 \text{ h}^{-1} \text{ Mpc}$  below. The upper limit  $16 \text{ h}^{-1} \text{ Mpc}$  actually is from the finite size of the simulation box.

For  $p > 1$ , the structure function decreases when the scale  $r$  increases from  $2$  to  $16 \text{ h}^{-1} \text{ Mpc}$ , while for  $p < 1$  it increases with the increase of scale  $r$ . This requires  $\xi(p) < 0$  for

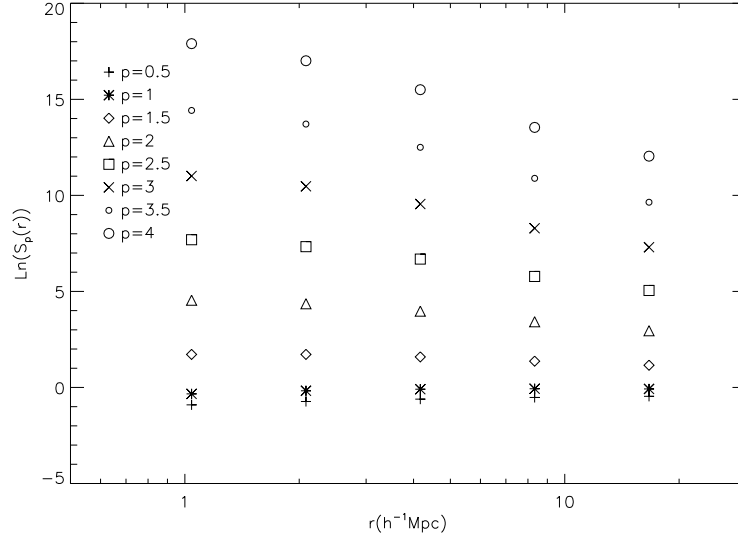


Fig. 2.— Structure functions  $S_p(r)$  vs.  $r$  in the range  $1 < r < 16 h^{-1}$  Mpc.  $p$  is equal to  $0.5 \times n$  and  $n = 1, 2 \dots 8$  from bottom to top.

$p > 1$ , and  $\xi(p) > 0$  for  $p < 1$ . Therefore, the intermittent exponent can't be fitted by  $\xi(p) \propto p$ . This is once again to show that the field is highly non-Gaussian. On the other hand, equation (7) does show that  $\xi(p)$  can have different signs for  $p > 1$  and  $p < 1$ .

### 3.2. Hierarchical relation and parameter $\beta$

We now test the hierarchical relation (11), which can be rewritten as

$$\ln F_{p+1}(r) = \beta \ln F_p(r) + A(r), \quad (13)$$

where  $A(r) = (1 - \beta) \ln F_\infty(r)$  depends only on  $r$ . Quantity  $A(r)$  may also depend on  $p$  if the proportional coefficient of relation (9) is  $p$ -dependent.

Equation (13) requires that  $\ln F_{p+1}(r)$  vs.  $\ln F_p(r)$  should be a straight line for a given scale  $r$ , and the slope  $\beta$  should be the same for all the scales  $r$ . Figure 3 presents the relations of  $\ln F_{p+1}(r)$  vs.  $\ln F_p(r)$  of the samples at  $z = 0$  for the scales  $r = 2.1, 4.2, 8.3$  and  $16.7 h^{-1}$  Mpc and for  $p = 1, 1.5, 2$ , and  $2.5$ . It shows that all the relations of  $\ln F_{p+1}$  vs.  $\ln F_p$  at different  $r$  can be well fitted by straight lines with slope  $\beta = 0.28 \pm 0.02$ .

Figure 3 also shows that  $A(r)$  depends only on  $r$ , but not on  $p$ . This is consistent with the assumption of the  $p$ -independence of the proportional coefficient of relation (9). If  $A(r)$



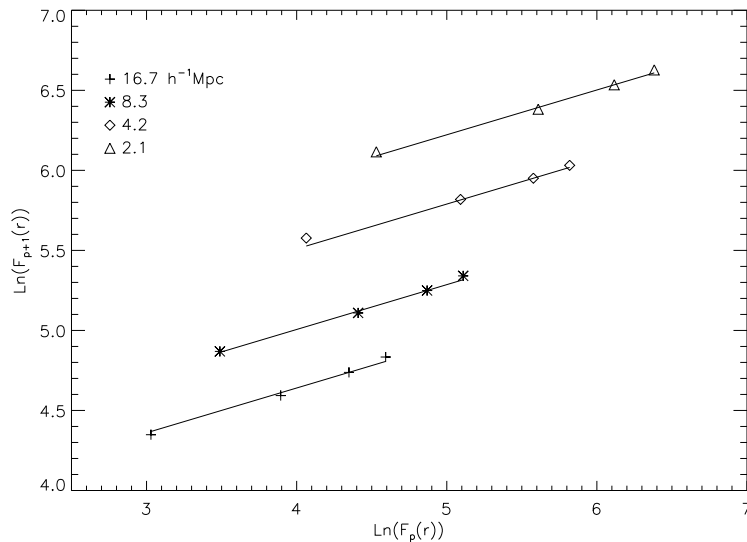


Fig. 3.—  $\ln F_{p+1}$  vs.  $\ln F_p$ .  $r$  is equal to 2.1, 4.2, 8.3, and  $16.7 \text{ h}^{-1} \text{ Mpc}$  for lines from top to bottom. In each lines, the four data points correspond to  $p = 1, 1.5, 2,$  and  $2.5$ .

is  $p$ -independent, we can find the following relation from eq.(13)

$$\ln[F_{p+1}(r)/F_3(r)] = \beta \ln[F_p(r)/F_2(r)]. \quad (14)$$

This is, for *all*  $r$  and  $p$ ,  $\ln[F_{p+1}(r)/F_3(r)]$  vs.  $\ln[F_p(r)/F_2(r)]$  should be on a straight line. The relation of equation (14) is tested in Figure 4. All data points can indeed be fitted by a straight line with slope 0.28. This is the hierarchy of the density fluctuations between different order  $p$  on various scale  $r$ .

### 3.3. Intermittent exponent and parameter $\gamma$

The intermittent exponent  $\xi(p)$  as a function of  $p$  can be measured by fitting  $S_p(r)$  (Figure 2) with a straight line of  $\ln S_p(r) = \xi(p) \ln r + \text{const}$  for each  $p$ . The measured  $\xi(p)$  for the sample at  $z = 0$  are shown in Figure 5. The error bars are the variance of  $\xi(p)$  over 100 samples, each of which contains 100 one-dimensional sub-samples.

Equation (7) shows that the shape of  $\xi(p)$  as a function of  $p$  depends only on parameter  $\beta$ , while parameter  $\gamma$  gives the overall amplitude of the curve  $\xi(p)$ . Since  $\beta$  is already determined in the last section, we can determine the parameter  $\gamma$  by fitting Equation (7) to the amplitude of the measured  $\xi(p)$ . The best fitting result is  $\gamma = 0.91$ . The fitted curve  $\xi(p)$  are also shown in Figure 5. It shows that the feature of the intermittent exponent  $\xi(p)$

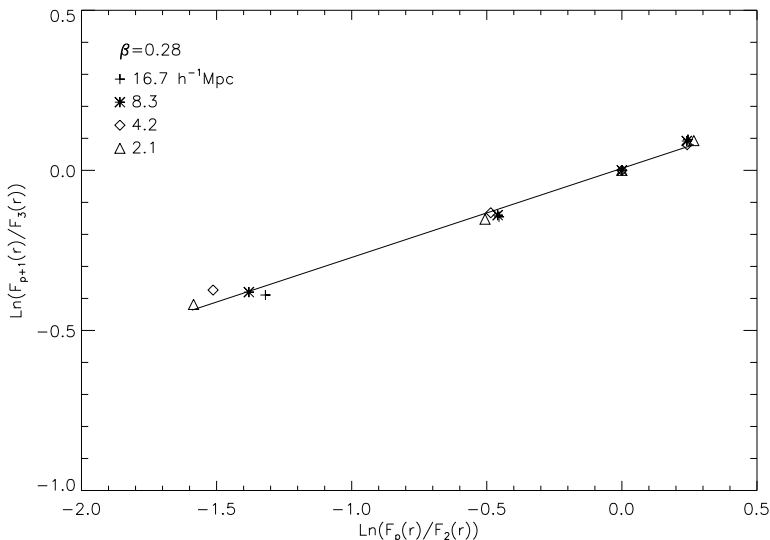


Fig. 4.—  $\ln[F_{p+1}(r)/F_3(r)]$  vs.  $\ln[F_p(r)/F_2(r)]$  for data points of  $r = 2.1, 4.2, 8.3$  and  $16.7 \text{ h}^{-1} \text{ Mpc}$  and  $p = 1, 1.5, 2, \text{ and } 2.5$ .

of the cosmic baryon fluid at  $z = 0$  in the range of  $0.5 \leq p \leq 6$  can be well reproduced with the log-Poisson model with parameters  $\beta = 0.28$  and  $\gamma = 0.91$ .

One can make a further test of parameter  $\gamma$  from equation (9). Since  $\beta = 0.28$ , we have  $(0.28)^3 \simeq 0.02 \ll 1$ , and then, equation (9) yields

$$\ln F_p(r) \simeq -\gamma \ln r + \text{const}, \quad \text{if } p > 3. \quad (15)$$

Equation (15) requires that the relations of  $\ln F_p(r)$  vs.  $\ln r$  should be straight lines for all orders  $p > 3$  with the same slope of  $\gamma$ . Figure 6 presents the relation between  $\ln F_p(r)$  and  $\ln r$ , which can be fitted by straight lines in the scale range of  $2 \leq r \leq 16 \text{ h}^{-1} \text{ Mpc}$ . The slope of the lines with  $p > 3$  are  $0.88 \pm 0.06$ , consistent with the value of  $\gamma = 0.91$  determined from  $\xi(p)$  (Figure 5).

### 3.4. Moments

With the determined parameters  $\beta$  and  $\gamma$ , we can predict statistical properties of the cosmic baryon fluid without other free parameters. As the first one, we consider the ratio between the high order and 2nd order moments,  $\langle \delta \rho_r^{2p} \rangle / \langle \delta \rho_r^2 \rangle^p$ . When  $p = 2$ , it is kurtosis, which is a popular tool to detect non-Gaussianity. For a Gaussian field, the ratio should be a constant, independent of  $r$ . The 2nd moment  $\langle \delta \rho_r^2 \rangle$  actually is the power spectrum of the

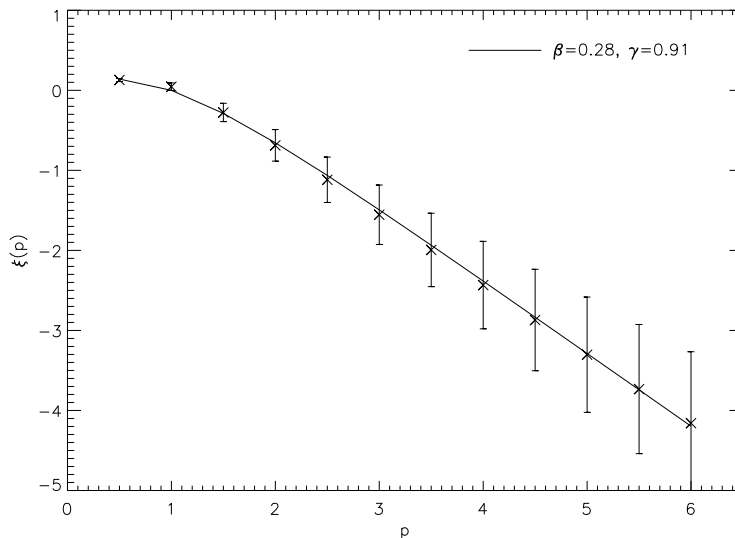


Fig. 5.— Intermittent exponent  $\xi(p)$ . The solid line is given by equation (7) with  $\beta = 0.28$  and  $\gamma = 0.91$ . The data points are from the fitting to the structure function  $S_p(r)$  with equation (7). The error bars are the variance of  $\xi(p)$  over 100 samples, each of which contains of 100 one-dimensional sub-samples.

mass density field (Fang & Feng 2000). For the log-Poisson model we have (see Appendix)

$$\ln \frac{\langle \delta \rho_r^{2p} \rangle}{\langle \delta \rho_r^2 \rangle^p} = K_p \ln r + \text{const} \quad (16)$$

with

$$K_p = -\gamma \frac{p(1 - \beta^2) - (1 - \beta^{2p})}{1 - \beta}. \quad (17)$$

That is,  $\ln(\langle \delta \rho_r^{2p} \rangle / \langle \delta \rho_r^2 \rangle^p)$  is linearly dependent on  $\ln r$  (scale free) with the coefficient  $K_p$  determined by  $\beta$  and  $\gamma$ . As expected, for Gaussian field ( $\beta \rightarrow 1$ ),  $K_p = 0$ , i.e., the ratio of moments is independent on  $\ln r$ .

Figure 7 shows the relation of  $\ln(\langle \delta \rho_r^{2p} \rangle / \langle \delta \rho_r^2 \rangle^p)$  vs.  $\ln r$  for the sample at redshift  $z = 0$ . For clarity, we show only the results of  $p = 2$  and  $3$ , which correspond to the statistical order 4 and 6. The errors are calculated as the variance over 100 samples, each of which contains 100 lines. Since the error bars actually are very small in logarithm scale, one can not show them in Figure 7. The solid lines of Figure 7 are given by a least square fitting and have slopes  $1.06 \pm 0.06$  and  $2.10 \pm 0.12$ , which are in agreement with the values  $1.07$  and  $2.23$  calculated from equation (17) with  $\beta = 0.28$  and  $\gamma = 0.91$ .

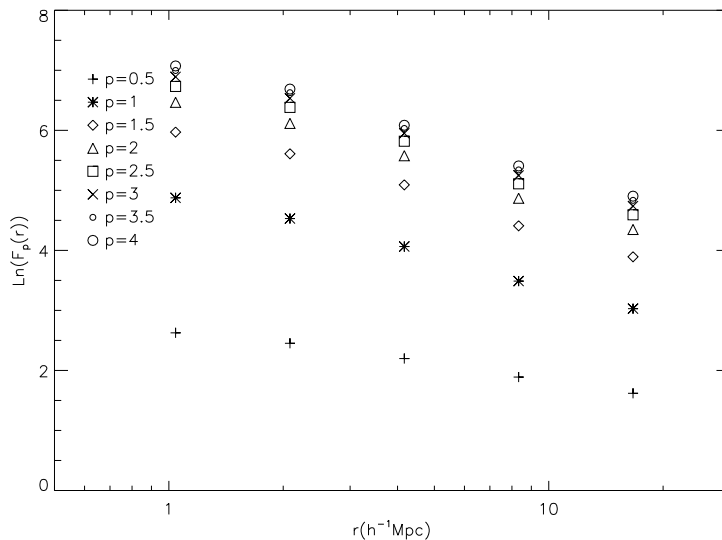


Fig. 6.—  $\ln F_p(r)$  vs.  $\ln r$  for  $p = 0.5$  to 4 from bottom to top.

### 3.5. Scale-scale correlation

A powerful non-Gaussian detector is the so-called scale-scale correlation, which is defined as

$$C_{r_1, r_2}^{p, p} \equiv \frac{\langle \delta \rho_{r_1}^p \delta \rho_{r_2}^p \rangle}{\langle \delta \rho_{r_1}^p \rangle \langle \delta \rho_{r_2}^p \rangle}. \quad (18)$$

Obviously, for a Gaussian field,  $C_{r_1, r_2}^{p, p} = 1$ . It has been shown that one can construct a non-Gaussian field, which has identical first and second order statistics as a Gaussian field, but has strong scale-scale correlation (Pando et al 1998).

It is especially important to measure the scale-scale correlation of cosmic baryon matter. The clustering of cosmic large scale structure in the nonlinear regime essentially is due to the interaction between Fourier modes on different scales (e.g., Peebles 1980). Therefore, cosmic clustering will definitely yield the transfer of the density perturbation powers between different scales, which leads to scale-scale correlation. Scale-scale correlation is also effective to distinguish various hierarchy cascade models (Pando et al. 1998). For instance, a Gaussian hierarchy cascade, like the model of Cole and Kaiser (1987), still yields  $C_{r_1, r_2}^{p, p} = 1$ , while the so-called  $p$ -model and  $\alpha$ -model yield  $C_{r_1, r_2}^{p, p}$  depending on both  $p$  and  $r$  (Greiner et al. 1996).

If the ratio  $r_2/r_1$  is fixed, the log-Poisson model predicts the scale-scale correlation to be (see Appendix)

$$C_{r_1, r_2}^{p, p} = B(r_2/r_1) r_1^{\xi(2p) - 2\xi(p)}, \quad (19)$$

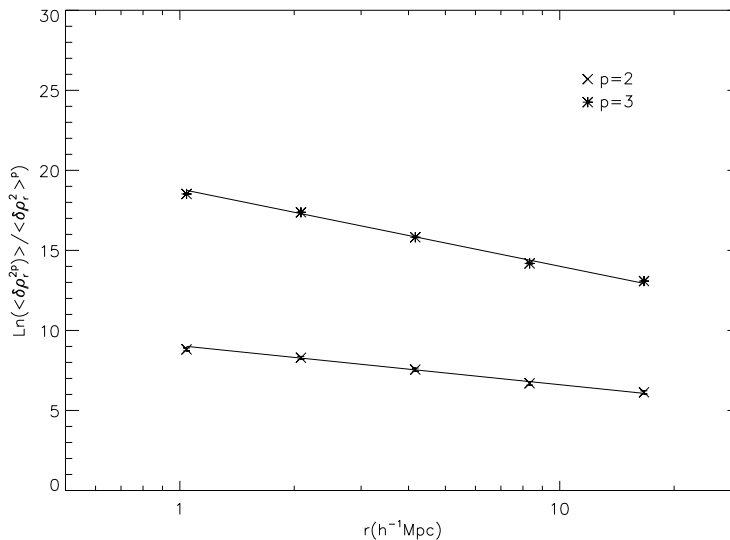


Fig. 7.— The ratio between high order and 2nd order moments  $\langle \delta \rho_r^{2p} \rangle / \langle \delta \rho_r^2 \rangle^p$  as a function of  $r$  for  $p = 2$  and 3. The solid lines are given by the least square fitting, which yields slopes consistent with the ones calculated from equation (17) with  $\beta = 0.28$  and  $\gamma = 0.91$ .

where the coefficient  $B(r_2/r_1)$  depends only on the ratio  $r_2/r_1$ , as the log-Poisson model is invariant of the dilation.

Thus, assuming  $r_2/r_1$  remains constant, the relationship of  $\ln C_{r_1, r_2}^{p, p}$  vs.  $\ln r_1$  should be a straight line with the slope  $\xi(2p) - 2\xi(p) = -\gamma(1 - \beta^p)^2 / (1 - \beta)$ . The result is shown in Figure 8, in which we take  $r_1/r_2 = 2$  and  $p = 2, 3$ . When the number  $p = 3$ , the statistics of equation (19) actually is of  $2p = 6$  order. Figure 8 shows that for  $r > 4h^{-1}\text{Mpc}$ , the scale-scale correlations can be well fitted by straight lines with slopes  $1.11 \pm 0.02$  and  $1.20 \pm 0.01$  for  $p = 2$  and 3, which are consistent with the values 1.10 and 1.20 calculated from eq.(19) with  $\beta = 0.28$  and  $\gamma = 0.91$ . The lower limit  $4 h^{-1}$  Mpc for the scale-scale correlation is higher than the lower limit  $2 h^{-1}$  Mpc of the statistics in previous sections. It is because we take  $r_2/r_1 = 2$ , and the scale-scale correlation of  $4 h^{-1}$  Mpc actually is the correlation between modes of 4 and 2  $h^{-1}$  Mpc.

#### 4. Evolution of $\beta$ and $\gamma$

We repeat the similar analysis for samples at redshifts  $z = 1, 2, 3$ , and 4. The non-Gaussian features of all these samples can also be well explained with the log-Poisson model. The parameters  $\beta$  and  $\gamma$  are listed in Table 1, which shows that both the parameters  $\beta$  and  $\gamma$

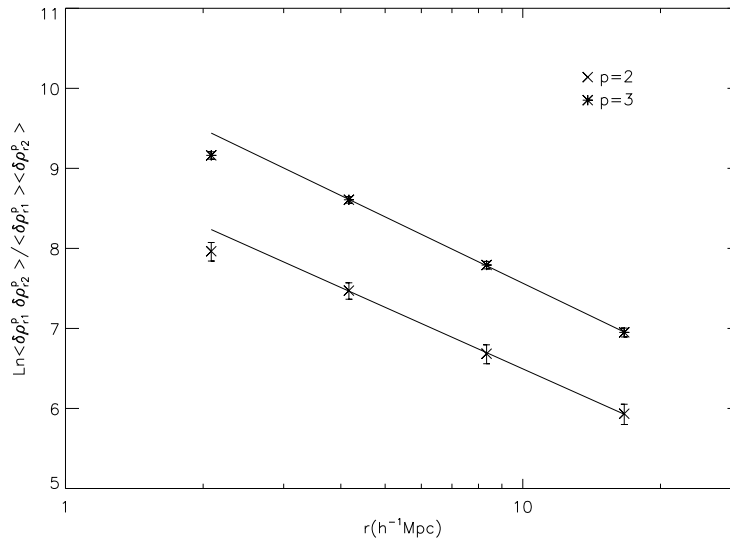


Fig. 8.— Scale-scale correlation of the sample at  $z = 0$  for  $p = 2$  and 3 with  $r_2/r_1 = 2$ .

The error bars are the variance over 100 samples, each of which contains of 100 lines.

are increasing with redshift. The increase of  $\beta$  with redshift indicates that the intermittency is stronger at lower redshifts, and the fields at higher redshifts contain less singular structures than that at lower redshifts.

On the other hand, the increase of  $\gamma$  with redshift indicates that the singular feature is even stronger at higher redshift. This probably is because the baryon fluid is significantly heated by the Burgers' shocks at lower redshift (He et al. 2004) and leads to weaker singular structures.

Table 1:  $\beta$  and  $\gamma$  at different redshift  $z$

$z$	0	1	2	3	4
$\beta$	0.28	0.34	0.34	0.38	0.43
$\gamma$	0.91	0.91	1.0	1.06	1.16

## 5. Discussion and conclusion

In the nonlinear regime of cosmic clustering, the dynamical behaviors of either dark matter or baryon fluid are complicated. Nevertheless, it is generally believed that the evolution should be scale-covariant in the range where the dynamical equations and initial perturbations are scale-free. Therefore, hierarchical and universal scaling relations have been widely used to describe the nonlinear clustering. For instance, the hierarchical relations of irreducible correlation functions and the universal density profile of halos are successful in the description of the statistical features of massive halos of dark matter.

However, it has already been recognized in the early study of cosmic structure formation that in the nonlinear regime the dynamical behavior of cosmic baryon doesn't always follow the collisionless dark matter. The non-Gaussianity of the mass and velocity fields of baryon fluid cannot be given by a similar mapping of the mass and velocity fields of dark matter. For instance, the halo model assumes that all mass fields are given by a superposition of the halos on various scales, and all non-Gaussian behaviors of the density field are described by the universal density profile (e.g., Cooray & Sheth 2002), this makes it difficult to explain the intermittency and the scale-scale correlation of the transmitted flux in the absorption spectra of QSOs.

We show that the evolution of the cosmic baryon fluid, governed by the Navier-Stokes equation in an expanding universe, is also hierarchical in the scale range in which the dynamical equations and initial perturbations are scale-free. The non-Gaussian behavior of the mass density field of baryon fluid can be well explained by the log-Poisson hierarchical cascade model. The SL formula and/or log-Poisson model are universal for the fully developed turbulence of Navier-Stokes fluid in the scale-free range. Therefore, the result of this paper implies that, in the scale-free range, the cosmic baryon fluid reaches a statistically quasi-steady state. For a fully developed turbulence, energy passes from large to the smallest eddies and finally dissipates into thermal motion, while the cosmic baryon fluid undergoes the evolution of clustering and finally falls into massive halos of dark matter to form structures, including light-emitting objects. Therefore, the log-Poisson model works on the scale range from the onset scale of the nonlinear evolution (a few tens of  $h^{-1}$  Mpc) to the dissipation scale, i.e., the Jeans length.

In view of this picture, one can say that in the nonlinear regime, the statistical properties of the cosmic baryon fluid are actually less dependent on the details of the dissipative processes. This property has already been noted in describing baryon matter by the Burgers' equation. Although the Burgers' equation contains a dissipative term, which leads to the formation of shocks and condense into luminous objects (Jones 1999), the self-similar properties of Burgers' turbulence actually depend very weakly on the dissipative term.

We now address the possible applications of the log-Poisson model. First, it is interesting to compare the log-Poisson model with the lognormal model, which assumes that the PDFs of the cosmic baryon matter is log-normal and no details of dissipative processes are needed (Bi & Davidsen 1997). The lognormal model is successful to explain some statistical features of Ly $\alpha$  forests and also predicts that the transmitted flux in the spectra of QSOs is non-Gaussian and intermittent. This result is qualitatively consistent with the observed data; however, non-Gaussian features given by the lognormal model do not quantitatively fit the observed data. For instance, the high order moment (§3.4) given by the lognormal model has a  $K_p \propto p(p-1)$ , while the data show  $K_p \propto -p^{0.1}(p-1)$  (Pando et al. 2002). The later is actually close to the log-Poisson model. Therefore, the higher order statistics of the Ly $\alpha$  transmitted flux would be able to discriminate between the log-Poisson and the lognormal model.

Second, recent studies have shown that the turbulence behavior of baryon gas can be detected by the Doppler-broadened spectral lines (Sunyaev et al. 2003; Lazarian & Pogosyan 2006). Although these works focus on the turbulence of baryon gas in clusters, the result is still applicable, at least, for the warm-hot intergalactic medium (WHIM), which is shown to follow the evolution of Burgers' fluid on large scales (He et al. 2004, 2005). The last but not least, the polarization of CMB is dependent on the density of electrons, and therefore, the map of CMB polarization would provide a direct test on the non-Gaussian features of ionized gas when the data on small scales becomes available.

J.L acknowledges the financial support of the International Center for Relativistic Astrophysics. This work is supported in part by the US NSF under the grant AST-0507340. We also thank Mr. Ding Ma for his contributions in the early stage of this project.

### A. Log-Poisson model and intermittency exponent

In this appendix we give the details of deriving the statistical properties of the log-Poisson cascade model. Let us consider the log-Poisson model

$$|\delta\rho_{r_1}| = W_{r_0r_1}|\delta\rho_{r_0}|, \quad (\text{A1})$$

where

$$W_{r_0r_1} = \beta^m(r_0/r_1)^\gamma, \quad (\text{A2})$$

and  $m$  is a Poisson variables with probability distribution function

$$P(m) = \exp(-\lambda_{r_0r_1})\lambda_{r_0r_1}^m/m!. \quad (\text{A3})$$



and

$$\lambda_{r_0 r_1} = \gamma[\ln(r_0/r_1)]/(1 - \beta). \quad (\text{A4})$$

Thus

$$\langle W_{r_0 r_1}^p \rangle = \sum_m (\beta^m (r_0/r_1)^\gamma)^p \exp(-\lambda_{r_0 r_1}) \lambda_{r_0 r_1}^m / m! \quad (\text{A5})$$

$$= \exp(-\lambda_{r_0 r_1}) (r_0/r_1)^{\gamma p} \sum_m \beta^{mp} \lambda_{r_0 r_1}^m / m! \quad (\text{A6})$$

$$= e^{-\lambda_{r_0 r_1}} e^{\gamma p \ln(r_0/r_1)} \sum_m (\beta^p \lambda_{r_1 r_2})^m / m! \quad (\text{A7})$$

$$= e^{-\lambda_{r_0 r_1}} e^{\gamma p \ln(r_0/r_1)} e^{\beta^p \lambda_{r_0 r_1}} \quad (\text{A8})$$

$$(\text{A9})$$

Using equation (A4), we have

$$\langle W_{r_0 r_1}^p \rangle = (r_0/r_1)^{-\xi(p)}, \quad (\text{A10})$$

with

$$\xi(p) = -\gamma[p - (1 - \beta^p)/(1 - \beta)]. \quad (\text{A11})$$

Therefore

$$\frac{S_p(r_1)}{S_p(r_2)} = \frac{\langle W_{r_0 r_1}^p \rangle}{\langle W_{r_0 r_2}^p \rangle} = \left(\frac{r_1}{r_2}\right)^{\xi(p)}. \quad (\text{A12})$$

For moments equation, we have

$$\frac{\langle \delta \rho_r^{2p} \rangle}{\langle \delta \rho_r^2 \rangle^p} = \frac{\langle W_{r_0 r}^{2p} \rangle}{(\langle W_{r_0 r}^2 \rangle)^p} = (r/r_0)^{\xi(2p) - p\xi(2)}. \quad (\text{A13})$$

Therefore,

$$\ln \frac{\langle \delta \rho_r^{2p} \rangle}{\langle \delta \rho_r^2 \rangle^p} = K_p \ln r + \text{const}, \quad (\text{A14})$$

and

$$K_p = \xi(2p) - p\xi(2) = -\gamma \frac{p(1 - \beta^2) - (1 - \beta^{2p})}{1 - \beta}. \quad (\text{A15})$$

For scale-scale correlation, we have

$$C_{r_1, r_2}^{p,p} = \frac{\langle \delta \rho_{r_1}^p \delta \rho_{r_2}^p \rangle}{\langle \delta \rho_{r_1}^p \rangle \langle \delta \rho_{r_2}^p \rangle} = \frac{\langle W_{r_0 r_1}^p W_{r_0 r_2}^p \rangle}{\langle W_{r_0 r_1}^p \rangle \langle W_{r_0 r_2}^p \rangle}. \quad (\text{A16})$$

Using equation (A10), if keeping  $r_1/r_2$  to be constant, the  $r_1$ -dependence of  $C_{r_1, r_2}^{p,p}$  is given by

$$C_{r_1, r_2}^{p,p} = A(r_2/r_1) r_1^{\xi(2p) - 2\xi(p)}. \quad (\text{A17})$$

## REFERENCES

- Bec, J. and Frisch, U. 2000, Phys. Rev. E61, 1395
- Benzi, R., Biferale, L. & Trovatore, E., 1996, Phys. Rev. Lett. 77, 3114
- Berera, A. and Fang, L.Z. 1994, Phys. Rev. Lett. 72, 458
- Bi, H.G. and Davidsen, A.F. 1997, ApJ, 479, 523
- Boldyrev, S., Nordlund, A. and Padoan, P. 2002, Phys. Rev. Lett. 89, 031102
- Cooray, A. and Sheth, R. 2002, Physics Reports, 372, 1
- Davoudi, J., Masoudi, A.A., Tabar, M.R., Rastegar, A.R. and Shahbazi, F. 2001, Phys. Rev. E63, 056308
- Dubrulle, B. 1994, Phys. Rev. Lett. 73, 959
- Fang, L.Z. and Feng, L.L. 2000, ApJ, 539, 5
- Fang, L.Z. and Thews, R. 1998, Wavelets in Physics, World Scientific (Singapore)
- Farge, M. 1992, Ann. Rev. Fluid Mech. 24, 395
- Feng, L.L., Pando, J., and Fang, L.Z., 2003, ApJ, 587, 487
- Feng, L.L., Shu, C.W., and Zhang, M.P. 2004, ApJ, 612, 1
- Frisch, U. 1995, Turbulence, Cambridge University Press
- Greiner, M., Gieseemann, J., Lipa, P. and Carruthers, P. 1996, Phys. C. 69, 305
- Gurbatov, S.N., Saichev, A.I., Shandarin, S. F., 1989, MNRAS236, 385
- He, P., Feng, L.L. and Fang, L.Z. 2004, ApJ, 612, 14
- He, P., Feng, L.L. and Fang, L.Z. 2005, ApJ, 623, 601
- He, P., Liu, J.R., Feng, L.L., Shu, C.W. and Fang, L.Z. 2006, Phys. Rev. Lett. 96, 051302
- Jamkhedkar, P., Zhan, H. and Fang, L.-Z. 2000, ApJ, 543, L1
- Jones, B.J.T. 1999, MNRAS307, 376
- Kim, B., He, P., Pando, J., Feng, L.L., and Fang, L.Z. 2005, ApJ625, 599

- Kolmogorov, A.N. 1941, Dokl. Akad. Nauk SSSR, 30, 9
- Lässig, M. 2000, Phys. Rev. Lett. 84, 2618
- Lazrian, A. and Pogosyan, D. 2006, ApJ, 652, 1348
- Liu, J., Jamkhedkar, P., Zheng, W., Feng, L. L., & Fang, L. Z. 2006, ApJ, 645, 861
- Matarrese, S. and Mohayaee, R. 2002, MNRAS329, 37
- Monin, A.S. and Yaglom, A.M. 1975, Statistical fluid mechanics: Mechanics of turbulence Vol 2, ( Cambridge MIT press).
- Padoan, P., Boldyrev, S., Langer, W. and Nordlund, . 2003, ApJ, 583, 308
- Pando, J., Lipa, p., Greiner, M. and Fang, L.Z., 1998, ApJ, 496, 9
- Pando, J., Feng, L.-L., Jamkhedkar, P., Zheng, W., Kirkman, D., Tytler, D., Fang, L.-Z., 2002, ApJ, 574, 575
- Peebles, P. J. E. 1980, The Large-Scale Structure of the Universe, Princeton University Press
- Polyakov, A.M., 1995, Phys. Rev. E52, 6183
- Shandarin, S.F. and Zeldovich, Ya. B. 1989, Rev. Mod. Phys. 61, 185
- Spergel, D.N. *et al.*, 2006, astro-ph/0603449
- She, Z.S. and Lévéque, E., 1994, Phys. Rev. Lett. 72, 336
- She, Z.S. and Waymire, E.C., 1995, Phys. Rev. Lett. 74, 262
- Sunyaev, R.A., Norman, M.L. and Bryan, G.L. 2003, Astronomy Letters, 2, 783
- Zheng, W., et al., 2004, ApJ, 605, 631